Integral Solution of Nonlinear Magnetostatic Field Problems

Aldo Canova and Maurizio Repetto, *Member, IEEE*

***Abstract*—This paper presents a procedure for using integrals to solve nonlinear magnetostatic field problems. An integral equation on magnetized volume, expressed in terms of magnetic field H or magnetization M, is discretized by means of edge elements on a tetrahedral mesh and solved numerically by means of a collocation method. The procedure approaches nonlinear by means of the fixed-point iterative technique. It sets up two different iterative schemes with complementary features. This paper gives details about implementation and presents and discusses results on some test cases.**

***Index Terms*—Edge elements, fixed-point nonlinear technique, integral equations, magnetostatics.**

I. Introduction

INTEGRAL formulations of electromagnetic equations have been extensively used in theoretical studies and in numerical analysis. They have always compared to differential formulations with respect to which they have advantages and drawbacks. Briefly, their main advantages in the numerical analysis of electromagnetic fields can be summarized in

1) discretization of the active regions of the problem only neglecting the surrounding space;
2) reduced number of unknowns;
3) high accuracy in the computation of fields outside the active regions;
4) possibility of decomposition of the problem domain and easy use of parallel computation.

On the contrary, their main drawbacks are

1) full interaction between all the unknowns in the problem, leading to a full matrix of coefficients;
2) presence of singular terms in the computation of coefficients requiring the computation volume integrals with high accuracy.

When three-dimensional (3-D) problems with intricate geometry are to be solved, issues 1) and 2) are particularly appealing, and this explains the relative success of integral-based analysis tools in electromagnetic applications.

Among integral formulations, volume and boundary treatment can be devised. Boundary integral methods can be efficently used in linear problems, and they realize the maximum reduction in number of unknowns requiring field variables only on the boundaries of the domain. On the contrary, they can deal only with regions containing homogeneous materials excluding thus nonlinear media where material properties vary from point to point. This reason explains the relative success of boundary integral techniques applied to electric field problems. In magnetic field problems, the need to deal with nonlinear materials is often found so that integral techniques based on volume discretization have been diffusely employed.

Several numerical field procedures have been proposed in the literature, and they have been extensively used since the 1970s [1]. Different approaches were used, such as changing the solution field variable, the way in which the domain was discretized, and the numerical method used for the solution. For instance, among the others, Trowbridge proposed an integral formulation based on magnetization vector and nodal elements solved by collocation method [2], while Albanese and Rubinacci devised a solution of the integral equation based on magnetic vector potential on edge elements and weighted residual approximation [3].

In this work, an integral formulation similar to that proposed by Kettunen and Turner [4] is adopted addressing in particular the problem of matrix coefficient computation (Section II) and nonlinear solution issue (Section III). Section IV is devoted to the discussion of the results obtained on some test cases.

II. Formulation of the Integral Equation

The formulation of the magnetostatic problem can be made by taking advantage of the usual magnetic field decomposition

$$\mathbf{H} = \mathbf{H}_c + \mathbf{H}_m \tag{1}$$

where $\mathbf{H}_c$ is the magnetic field created by imposed current sources, and $\mathbf{H}_m$ is the magnetic field created by magnetization of ferromagnetic media.

While the first term can be obtained by integrating the Biot-Savart law on the volume of current sources, the second one can be obtained by a volume integral over the magnetized bodies

$$\mathbf{H}_m(\mathbf{r}) = -\frac{1}{4\pi}\nabla_f \left(\int_\Omega \mathbf{M} \cdot \nabla_s \left(\frac{1}{|\mathbf{r}_f - \mathbf{r}_s|} \right) d\Omega \right) \tag{2}$$

where

Ω	region of ferromagnetic material;
$\mathbf{r}_f$ and $\mathbf{r}_s$	position vector of field and source points, respectively; the gradient inside the volume integral acts on source points, while the external one acts on field points;
$\mathbf{M}$	magnetization.

Manuscript received July 19, 2000; revised January 29, 2001.

The authors are with the Politecnico di Torino, Dipartimento di Ingegneria Elettrica Industriale, Torino, Italy (e-mail: canova@polel1.polito.it; repetto@polel1.polito.it).

Publisher Item Identifier S 0018-9464(01)03509-9.

In linear magnetic problems, by introducing magnetic susceptibility χ, a solution scheme can be obtained by (1), and the equation becomes

$$\mathbf{H} = \mathbf{H}_c - \frac{1}{4\pi}\nabla_f \left(\int_\Omega \chi \mathbf{H} \cdot \nabla_s \left(\frac{1}{r} \right) d\Omega \right)$$
$$\Rightarrow \mathbf{H} + \frac{1}{4\pi}\nabla_f \left(\int_\Omega \chi \mathbf{H} \cdot \nabla_s \left(\frac{1}{r} \right) d\Omega \right) = \mathbf{H}_c \quad (3)$$

where, for brevity, r is the distance between source and field point.

The integral equation can be solved for magnetic field $\mathbf{H}$ by discretizing the region of magnetized materials. Several approaches have been presented in the literature. Discretization by means of piecewise constant shape functions [5], [6], discretization by means of nodal element formulating magnetic field H by means of magnetic scalar potential [2], and discretization using edge elements [4]. This last approach has been considered very efficient since it formulates directly the problem in terms of field quantities, and because of the basic properties of the edge elements (conservation of tangential component of field), it imposes a high degree of regularity to the field and thus has been adopted in this procedure.

A. Edge Elements

Edge elements have been widely used in computational electromagnetism since their introduction in the research community by Albanese and Rubinacci [7] and by Bossavit [8]. Without going through details about properties of edge elements that can be found for instance in [7], we state here some definitions. Given a tetrahedron of vertices $\{\alpha, \beta, \gamma, \delta\}$ for the generic kth edge of the tetrahedron $\{\alpha, \beta\}$, a shape function can be defined as

$$\mathbf{w}_k = (N_\alpha \nabla N_\beta - N_\beta \nabla N_\alpha) l_{\alpha\beta} \quad (4)$$

where N_α and N_β are the nodal shape functions of nodes α and β, respectively, and $l_{\alpha\beta}$ is the length of the edge.

Interpolation of magnetic field $\mathbf{H}$ can be achieved inside the element by means of

$$\mathbf{H} = \sum_{k=1}^{6} h_k \mathbf{w}_k \quad (5)$$

where h_k is the tangential component of magnetic field along the kth edge of the tetrahedron. In the general case, six degrees of freedom are thus defined for each element.

B. Gauging of Solution

Under magnetostatic conditions and in the hypothesis that the region under analysis is simply connected, it can be easily shown that not all the projections of magnetic field along edges are linearly independent. Imposing in fact, that the circulation of $\mathbf{H}$ would be null on any closed curve contained inside the region, several constraints can be imposed on the solution. Topologically, the only degrees of freedom linearly independent are those lying on a tree of the mesh, that is, a path through mesh edges connecting all the nodes of the mesh but closing no loop [5]. This hypothesis allows to drastically reduce the number of linearly independent unknowns, from the total number of edges in the mesh to the number of nodes minus one, typically with usual 3-D mesh generators, this reduction is of almost one order of magnitude.

The knowledge of the tree tangential components allows one to reconstruct by means of linear operations the value of any tangential projection along the sides of the mesh and thus, it imposes no limitations on the reconstruction of the field.

Choice of the tree in the mesh is not univocal. In this case, a "breadth first" algorithm for tree determination [9] has been adopted since this would guarantee the shortest co-tree path.

C. Computation of Coefficients

Once the discretization of the domain has been performed and a tree along the edges of the mesh has been selected, the discretised form of (3) can be written as

$$([A] + [I])\{h\} = \{h_c\} \quad (6)$$

where

- $[I]$ unit matrix;
- $\{h\}$ array of tangential components of $\mathbf{H}$ along the tree branches;
- $\{h_c\}$ array of tangential components of magnetic field created by imposed source currents;
- $[A]$ matrix of coefficients.

The terms of matrix $[A]$ represent the interaction between tree edges in the mesh. Its coefficients can be computed by exploiting (3).

By considering an edge k between nodes α and β, the tangential component of magnetic field h_k due to magnetization along the edge is given by

$$h_k = \frac{\Phi_\beta - \Phi_a}{l_{\alpha\beta}} \quad (7)$$

where Φ_α and Φ_β are the reduced magnetic scalar potential values in α and β, and $l_{\alpha\beta}$ is the length of the side. Magnetic scalar potential as function of magnetization can be written as

$$\Phi = -\frac{1}{4\pi} \int_\Omega \chi \mathbf{H} \cdot \nabla \left(\frac{1}{r} \right) d\Omega. \quad (8)$$

By using the divergence theorem, the volume integral can be expressed by a surface integral [12]. Thus, (8) can be rewritten as

$$\Phi = -\frac{1}{4\pi} \int_{\partial\Omega} \frac{\chi \mathbf{H} \cdot \mathbf{n}}{r} d\Gamma \quad (9)$$

where $\mathbf{n}$ is the normal vector to the face. The contribution of the ith edge with magnetic field h_i on the edge k between nodes α and β can be written as

$$\gamma_{ki} = \frac{1}{4\pi} \left(\int_{\partial\Omega_i} h_i \chi \frac{\mathbf{w}_i \cdot \mathbf{n}}{r_\beta} d\Gamma - \int_{\partial\Omega_i} h_i \chi \frac{\mathbf{w}_i \cdot \mathbf{n}}{r_\alpha} d\Gamma \right) \quad (10)$$

where

- $\mathbf{w}_i$ edge shape function of edge i;
- $\partial\Omega_i$ surface obtained by the union of all the faces of the tetrahedra belonging to the support area of ith edge, that is, the region where its shape function is different from 0;

r_α and r_β distance between source point and points α and β, respectively.

The computation of terms γ_{ki} involves the integration of singular functions. The singularity happens only when potential is computed on the same node of the edge under consideration. Even in the case of nonsingular integrals, the coefficient has to be integrated in accurate way otherwise the quality of the whole solution is spoiled. In our case, coefficients are computed in three different ways depending on their degree of singularity.

1) Singular Coefficients: In this case, the analytical expression of the integral is computed. This can be done by means of a coordinate transformation with the new coordinate system having the origin coincident with the singular point and the new z' axis orthogonal to the face of the tetrahedron on which coefficient of (10) is computed. Details on the analytical expression of the singular integrals are given in the Appendix.

2) Near-Singular Coefficients: Expression obtained for the singular coefficient is valid only on tetrahedra that have a singular vertex. If the tetrahedron on which an integral of (10) is computed has no singular vertex but is very close to the singular point, its contribution is significant and critical to evaluate, but no analytical expression of contribute can be obtained. In these cases, the integral over the faces of the tetrahedron is computed accurately by means of quadrature formulas. In order to use adaptive quadrature rules following the Kronrod scheme [10], each triangular face of the tetrahedron is subdivided in four quadrilaterals and then a two-dimensional (2-D) quadrature rule is applied, as sketched in Fig. 1. This scheme is applied to all tetrahedra belonging to the first layer of elements around the singular point.

3) Regular Coefficients: For all the elements not belonging to the two previous classes, the computation of the coefficients is made by surface integrals on the triangular faces of the tetrahedron using a seven points quadrature rule specially devised for triangular patches [12].

4) Use of Symmetries: The possible presence of geometrical and supply symmetries in the domain under consideration can be exploited to reduce the number of unknowns in the problem. In fact, only the fundamental part of the problem must be discretized. Contributions of the symmetrical parts can be reconstructed by means of simple geometrical operations like translation, rotation, etc. This operation reduces the number of unknowns and reduces, in some cases, a multiply connected problem to a simply connected one. Nevertheless, all the integral contributes to the magnetic fields coming from symmetrical copies of the reduced domain have to be calculated. Since matrix coefficients computation is by large the most computational intensive part of the solution, the reduction in computational burden of the solution process is often negligible.

D. Matrix Assembly

The computation of coefficients γ_{ki} has to be performed considering as sources all the edges of the mesh but as target of the computation only the edges belonging to the tree selected for the solution.

Operatively, if n is the total number of the edges of the mesh and m the number of branches of the tree, a matrix $n \times m$ $[R]$ is built, each row of which corresponds to the contributes of one edge of the mesh, while each column corresponds to one edge belonging to the tree.

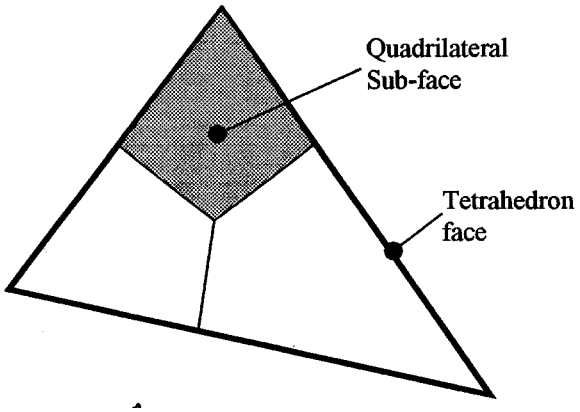

Fig. 1. Decomposition of triangular face in three quadrilateral domains.

After matrix $[R]$ has been built, the contributions of the co-tree edges are inserted in the square matrix $[A]$, which is $m \times m$, by taking into account that in discrete form

$$\oint_\lambda \mathbf{H} \cdot d\mathbf{l} = 0 \Rightarrow \sum_k h_k l_k = 0 \tag{11}$$

where λ is a closed path along mesh edges. For each co-tree edge, it can thus be written

$$h_i = \frac{1}{l_i}\left(-\sum_p h_p l_p\right) \tag{12}$$

where i is the generic co-tree branch, and the sum is extended to all the branches of the tree connecting the two extrema of ith edge. In this way, the magnetic field created by the ith edge on the kth branch of the tree can be attributed to the edges appearing in (12), that is

$$\gamma_{ki} h_i = \sum_p \left(-\frac{l_p}{l_i}\gamma_{ki}\right) h_p = \sum_p a_{kp} h_p. \tag{13}$$

Coefficients a_{kp} must be added to form matrix $[A]$.

E. Contribution of Permanent Magnets

If some part of the discretised region is aimed by a permanent magnetization, its contribution to the magnetic field has to be computed and added to the known term of the equation.

By considering a linear permanent magnet material, characterized by the material relation

$$B = \mu_0 \mu_{cr}(H - H_c) \tag{14}$$

where H_c is the coercive field, and μ_{cr} is the recoil relative permeability of the material given by $\mu_{cr} = B_r/(H_c\mu_0)$ with B_r the remanent magnetic flux density; magnetization can be written as

$$\begin{aligned} &\mathbf{B} = \mu_0\mathbf{H} + \mu_0\mathbf{M} = \mu_0\mu_{cr}(\mathbf{H} - \mathbf{H}_c) \\ &\quad \Rightarrow \mathbf{M} = (\mu_{cr} - 1)\mathbf{H} - \mu_{cr}\mathbf{H_c} = \chi_c\mathbf{H} - \mu_{cr}\mathbf{H_c} \end{aligned} \tag{15}$$

where χ_c is the reluctivity of the permanent magnet material. Inserting magnetization $\mathbf{M}$ of (15) in (3) gives rise to two contributes: one like γ_{ki} of (10) and a known term depending on H_c.

This contribution is due to magnetization of volume element, so that right hand side of tree edge k has the term

$$\gamma_k^{(E)} = \frac{1}{4\pi}\left(\oint_{\partial\Omega_E} \frac{\mathbf{H}_c \cdot \mathbf{n}}{r_\beta}\, d\Gamma - \oint_{\partial\Omega_E} \frac{\mathbf{H}_c \cdot \mathbf{n}}{r_\alpha}\, d\Gamma\right) \quad (16)$$

where $\gamma_k^{(E)}$ is the contribute of generic tetrahedron E on edge, k, $\mathbf{H}_c$ is the coercive field known as absolute value and spatial direction by the data of the problem, and other symbols have the same meaning of those of (10).

F. Thin Shell Elements

When thin ferromagnetic parts are contained inside the domain of the problem, some hypotheses can be made on their magnetization distribution. This situation can happen, for instance, when shielding of magnetic field is made by mean of thin ferromagnetic sheets. In fact, if the thickness of a ferromagnetic sheet is small with respect to its other dimensions, it is usually considered, see for instance [14], that the magnetic field inside the sheet is mainly directed parallel to its surface, or in other words, the component of magnetization normal to the sheet is negligible. In this case, considering Fig. 2, tangential components of magnetic field along edge k connecting nodes α and β on opposite sides of the sheet is null. Tetrahedral mesh degenerates thus in a triangular one with nodes α and β cohaleshing in one single node. Volume integrals become surface integral with thickness of the sheet δ as a multiplying factor. Edge element interpolation can be used as well in this case on 2-D surfaces while surface integrals of (9) become line integrals on the triangular element sides. The contribution of triangle surface is null because in this case $\mathbf{M} \cdot \mathbf{n} = 0$. A part from these peculiarities, that makes the solution process easier and faster with respect to a volume discretization of the sheet, all the other main features of the solution process stay the same.

III. Nonlinear Formulation

As the solution process in the linear case is naturally obtained by the integral (3), nonlinear solution requires the set-up of a nonlinear solution scheme which can give efficient answers to the problem.

A. Fixed Point Nonlinear Scheme

The well known fixed point (FP) nonlinear solution scheme, often referred to as Picard-Banach fixed point scheme, has been extensively used in the solution of nonlinear magnetic field problems since its introduction by Hantila in the 1970s [14], [15]. In summary, this technique represents a nonlinear curve by means of a linear characteristic of fixed slope and a nonlinear residual. This method has been often seen as an alternative to the more classic Newton-Raphson nonlinear scheme with respect to which it has complementary features [16].

According to the FP scheme, the working point of the nonlinear system can be found by iteratively updating the nonlinear residual. The method is proved to converge to the true solution under the hypothesis of nonlinear characteristic Lipshitz continuous and strongly monotone. These hypotheses are usually accomplished by all magnetic nonlinear curves. Optimal choice of the constant slope characteristic can be made according to maximum and minimum slopes of the nonlinear curve [17]. When used in conjunction with a numerical method that requires the solution of a linear system of equation, FP works better with direct solvers since solution matrix can be factorized once for all and the iterative process requires only the updation of the known term of the equation.

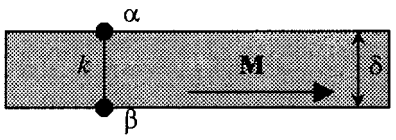

Fig. 2. Thin shell ferromagnetic element.

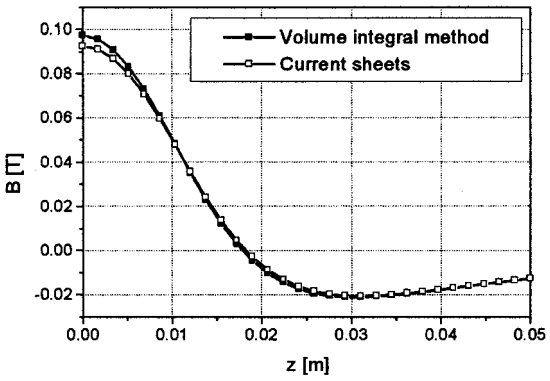

Fig. 3. Comparison of absolute value of flux density on the axis of the magnet.

Applied to the integral equation, FP method can generate two schemes: one formulated in terms of $\mathbf{H}$ and one formulated in terms of $\mathbf{M}$.

B. Solution in $\mathbf{H}$

Given a nonlinear characteristic $M = M(H)$ by means of FP, it can be written as

$$M(H) = \chi_{\mathrm{FP}} H + S \quad (18)$$

which gives rise to the following iterative scheme

$$S^{(i+1)} = M\left(H^{(i)}\right) - \chi_{\mathrm{FP}} H^{(i)} \quad (19)$$

where χ_{FP} is the FP constant, and i is the iteration index. Substituting magnetization inside (3), it becomes

$$\begin{aligned} &\mathbf{H} + \frac{1}{4\pi}\nabla\left(\int_\Omega (\chi_{\mathrm{FP}}\mathbf{H} + \mathbf{S}) \cdot \nabla\left(\frac{1}{r}\right) d\Omega\right) = \mathbf{H}_c \\ &\Rightarrow \mathbf{H} + \frac{1}{4\pi}\nabla\int_\Omega (\chi_{\mathrm{FP}}\mathbf{H}) \cdot \nabla\left(\frac{1}{r}\right) d\Omega \\ &= \mathbf{H}_c - \frac{1}{4\pi}\nabla\left(\int_\Omega \mathbf{S} \cdot \nabla\left(\frac{1}{r}\right) d\Omega\right). \end{aligned} \quad (20)$$

Equation (20) can be computed numerically as (3), taking into account the following. Matrix $[A]$ of (6) must be evaluated using FP constant χ_{FP}, and the integral term on the RHS must be computed starting from the residual obtained at the previous equation following the iterative scheme of (19). If residual $\mathbf{S}$ is expressed in terms of edge shape functions as magnetic field $\mathbf{H}$, its volume integral can be efficiently computed starting from

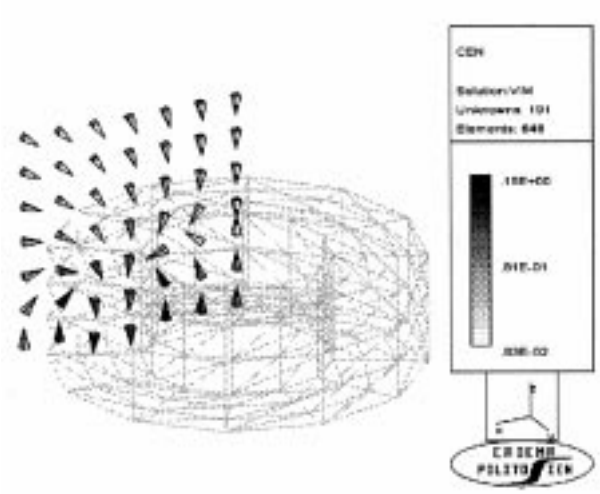

Fig. 4. Vector plot of magnetic flux density around the magnet.

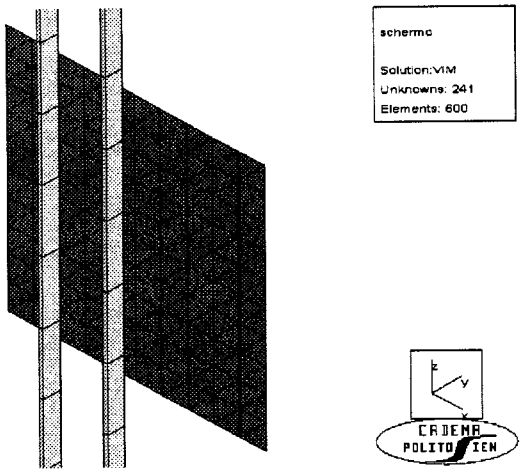

Fig. 5. Geometry of the test case for thin magnetic shields.

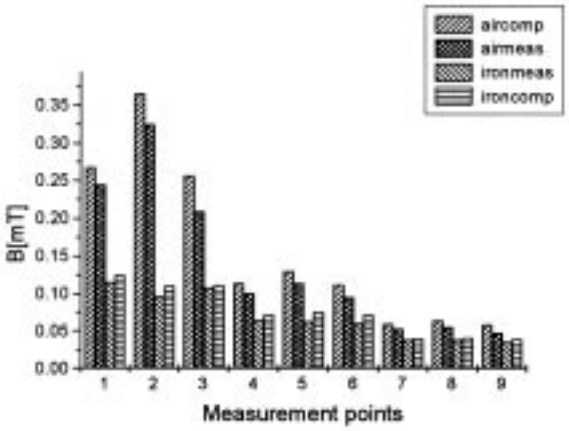

Fig. 6. Comparison of measured and computed magnetic flux desnity values with and without shield on nine reference points.

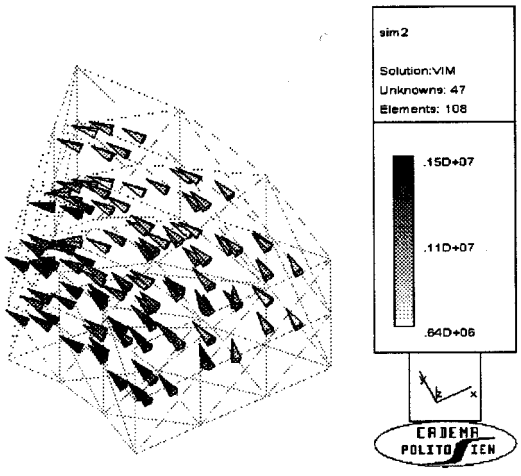

Fig. 7. Geometry of 1/8th of the nonlinear test case.

the coefficients γ of (10). In fact, considering that $\mathbf{M}, \mathbf{H}$ and $\mathbf{S}$ are lying on the same direction, knowing the value of $\mathbf{H}$ on each edge, for instance in its midside point, absolute value of $\mathbf{S}$ can be computed by means of (19), and the its projection along the edge can be obtained. Unfortunately, only tangential component of $\mathbf{H}$ is known on the edge, so that complete vector $\mathbf{H}$ must be evaluated by means of some higher order interpolation, for instance by averaging all the contributes to magnetic field $\mathbf{H}$ on one edge coming by all the tetrahedra sharing the edge, as it is usually done in first order finite element computations. Once the array $\{s\}$ of all the tangential projection of $\mathbf{S}$ on the edges has been computed, row-column product of $\{s\}$ times matrix $[R]$ introduced in previous chapter gives the integral term.

Term $\mathbf{S}$ is in general not irrotational. Thus, its value must be computed on all mesh edges and not only on tree ones. In this case, in fact, we cannot use (11) and (12), as we have done with $\mathbf{H}$. Anyway, the knowledge of matrix $[R]$, which contains the contributes of each mesh edge on tree edges, allows us to perform the integration quickly.

Schematically, the iterative scheme can be summarized in the following points:

1) computation of matrices $[R], [A]$ using χ_{FP};
2) factorization of matrix $[A]$;
3) solution of linearised equation;
4) computation of $\mathbf{H}$ on all edges of the mesh and evaluation of residual $\mathbf{S}$;
5) row-column product of $\{s\}$ times $[R]$;
6) assembly of the new RHS by summing $\{h_c\}$ and residual contribute;
7) backward substitution;
8) convergence otherwise go back to point *3)*.

C. Solution in $\mathbf{M}$

If the FP scheme is used to linearize the characteristic $H = H(M)$, a new scheme can be obtained as

$$H(M) = \xi_{\mathrm{FP}} M + W \tag{21}$$

$$W^{(i+1)} = H\left(M^{(i)}\right) - \xi_{\mathrm{FP}} M^{(i)} \tag{22}$$

where FP constant ξ_{FP} is the inverse of a susceptibility, and W is the residual term. In general, the curve $H = H(M)$ does not satisfy the hypothesis of Lipschitz continuity because in complete saturation conditions, the slope of the curve rises to infinity. Actually, these conditions are seldom reached in practical applications but anyway the characteristic must be truncated before reaching saturation.

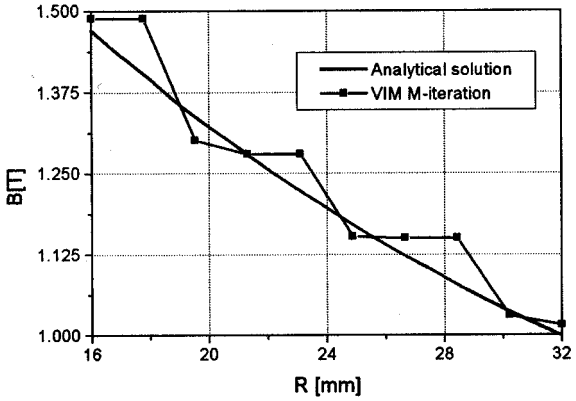

Fig. 8. Behavior of magnetic flux density along one radial direction in the nonlinear test case: analytical solution versus volume integral method.

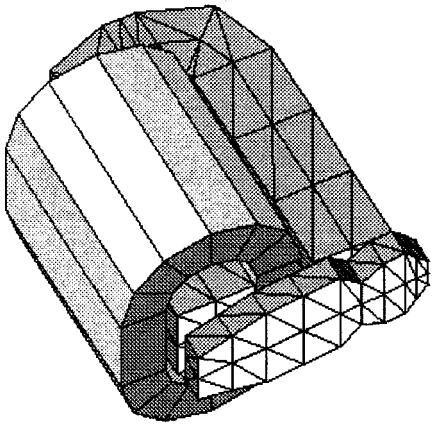

Fig. 9. Geometry of the nonlinear electromagnetic actuator.

Inserting (21) in (3) it comes out that

$$\xi_{\mathrm{FP}}\mathbf{M}+\mathbf{W}+\frac{1}{4\pi}\nabla\left(\int_{\Omega}\mathbf{M}\cdot\nabla\left(\frac{1}{r}\right)d\Omega\right)=\mathbf{H}_c$$

$$\xi_{\mathrm{FP}}\mathbf{M}+\frac{1}{4\pi}\nabla\left(\int_{\Omega}\mathbf{M}\cdot\nabla\left(\frac{1}{r}\right)d\Omega\right)=\mathbf{H}_c-\mathbf{W}. \quad (23)$$

The discretized form of (23) can be obtained by expressing magnetization $\mathbf{M}$ in terms of edge elements and by building the solution matrix with the FP constant ξ_{FP}.

In this case, $\mathbf{W}$ is a rotational vector field that can be interpreted as a magnetizing current $\mathbf{J}_m=\nabla\times\mathbf{M}$, which is added to the imposed current source. In this case, it is sensible to use an edge element for interpolating $\mathbf{M}$ because magnetization is split in an irrotational part that can be approximated on tree edges only and a rotational part that is constituted by the residual $\mathbf{W}$ which, as it was for $\mathbf{S}$, is computed on all mesh edges.

Again, the evaluation of residual term $\mathbf{W}$ requires us to know the magnetization $\mathbf{M}$ along the edges so an averaging of the solution similar to that previously described can be obtained. This time, the residual term does not need to be integrated on the volume. The solution procedure is made up of the following steps:

1) computation of matrices $[R],[A]$ using ξ_{FP};
2) factorization of matrix $[A]$;
3) solution of linearized equation;
4) computation of M on all edges of the mesh and evaluation of residual W on tree branches;
5) assembly of the new RHS by summing $\{h_c\}$ and residual contribute;
6) backward substitution;
7) convergence otherwise go back to point 3).

IV. Results on Test Cases

The proposed procedure has been applied to the analysis of different test cases, in the following, they will be briefly described and results discussed.

A. Permanent Magnet Case

A "pancake" permanent magnet for laboratory purposes has been analyzed in order to test the accuracy of the method. The torus has an inner radius of 1.6 cm and an external one of 3, 2 cm and has axial magnetization. The magnet is made of ferrite characterized by a residual induction of 0.4 T and a coercive field of 100 kA/m. The results of the volume integral method have been compared with a current sheet approximation of the permanent magnet material. In Fig. 3, the comparison of magnetic flux density values along the axis of the magnet obtained by the two techniques is shown and a very good agreement between the two sets of results can be appreciated. In Fig. 4, a

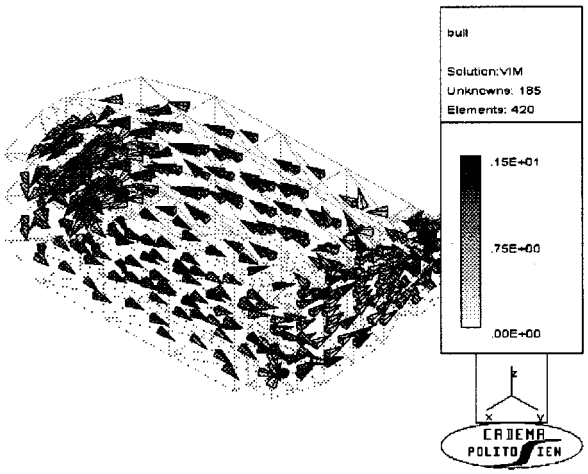

Fig. 10. Vector plot of magnetic flux density inside the electromagnetic actuator.

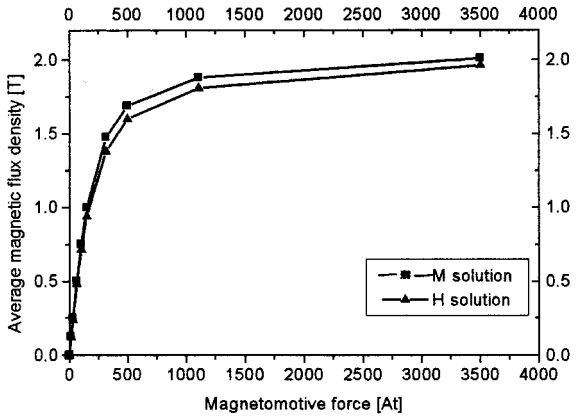

Fig. 11. Behavior of magnetic flux density versus magnetomotive force in the electromagnetic actuator.

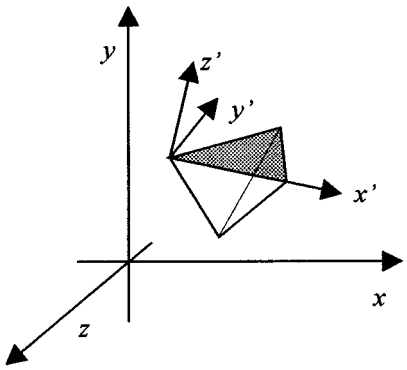

Fig. 12. Reference frames of the singular case.

vector plot of the magnetic flux density around the magnet is displayed.

B. Ferromagnetic Shields

The thin sheet approximation of the integral method is tested against measurements performed on a specially devised set-up for shielding efficiency evaluation. In this experimental set-up [18] plane ferromagnetic sheets can be interposed between a busbar system and a set of measurement points. In our case, a 60 × 60 cm sheet of GO material 0.3 mm thick was used, geometry is shown in Fig. 5. In Fig. 6, the comparison between experimental and simulated data is reported and again a satisfactory agreement is obtained.

C. Nonlinear Case With Analytical Solution

In order to test the performances of the nonlinear solver, a test case with a nonlinear analytical solution was used. This case, made of a hollow cylinder with a current carrying conductor along its axis, has a known solution. In fact, the structure presents no air gaps and due to the absence of demagnetizing effects, the magnetic field created by the magnetization of the ferromagnetic material is null. Magnetic field created by currents can be easily computed due to the simple geometry. This test case is also quite efficient for assessing the accuracy of matrix computation since in this case, the contribute $\mathbf{H_m}$ should be exactly zero. When applied to nonlinear materials, the problem gives an analytical nonlinear solution of magnetic field [17]. In this case, by taking advantage of symmetries present in the structure, only one eighth of the cylinder was discretized as shown in Fig. 7. In Fig. 8, the comparison between numerically computed and analytical solution in the case of heavy saturation is shown, showing the convergence of the method to the true solution. It must be noted that, since H is known in this particular structure, only M-iteration can be used because the H one is trivial.

D. Nonlinear Electromagnet

A nonlinear electromagnet for high dynamic applications was analyzed by means of the volume integral method. The geometry of the electromagnet is shown in Fig. 9, while in Fig. 10, the vector plot of magnetic flux density is shown. In this case, both nonlinear schemes could be used and results on average magnetic flux density values versus magnetomotive force in the maximum gap situation are shown in Fig. 11. As it can be seen, the two sets of results are quite close to each other. H-iteration scheme seems to always give results a little bit higher than those of the M-iteration. This behavior was obtained also in other configurations even if it is not clear if this would be a general behavior of the techniques.

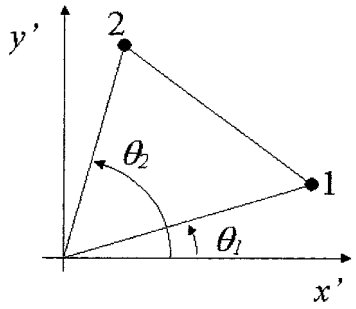

Fig. 13. Integration domain of the singular contribution.

V. Conclusion

An integral formulation for magnetostatic nonlinear problems has been presented and implemented in a numerical code. The magnetostatic problem is solved in terms of field variables that are expressed by means of edge element shape functions. The nonlinear problem is solved by means of the well known fixed point technique with two different expressions of the field variables both in terms of magnetic field and magnetization. The results obtained in some test cases show a good agreement with other computational techniques and measurements. Future work will continue trying to extend the formulation to time-varying cases.

Appendix

The computation of singular integral of (10) can be performed in an analytical way by means of a coordinates transformation. If a face of tetrahedron is considered, a new reference frame is set with the origin in the singular point and z' axis along the normal to the face (external to the element) as shown in Fig. 12.

By considering that the normal component of edge shape function contained in (10), it is expressed by linear terms

$$\mathbf{w} \cdot \mathbf{n} = Ax' + By' + Cz' + D \tag{A.1}$$

where A, B, C and D are constants, and the integral term can be expressed as

$$I = \int_{\theta_1}^{\theta_2} \int_0^{r(\theta)} \frac{Ar\cos\theta + Br\sin\theta + D}{r}\, dr\, d\theta \tag{A.2}$$

where $r\cos\theta$ and $r\sin\theta$ are the expression of x' and y' in polar coordinates, while z' term is null because of the special orientation of the new coordinate system and the other symbols have the meaning shown in Fig. 13.

By expressing in polar coordinates the straight line passing through points 1 and 2, the integral term becomes

$$I = \int_{\theta_1}^{\theta_2} \int_0^{\frac{K}{H\cos\theta + L\,\mathrm{sen}\,\theta}} (Ar\cos\theta + Br\sin\theta + D)\, dr\, d\theta \tag{A.3}$$

where

$$\begin{aligned} K &= x_1' y_2' - x_2' y_1'; \\ H &= y_2' - y_1'; \\ L &= x_1' - x_2'. \end{aligned}$$

Integrating on r coordinate, the integral becomes

$$I = \int_{\theta_1}^{\theta_2} \left[\frac{K^2(A\cos\theta + B\,\mathrm{sen}\,\theta)}{2(H\cos\theta + L\,\mathrm{sen}\,\theta)^2} + \frac{DK}{H\cos\theta + L\,\mathrm{sen}\,\theta} \right] d\theta. \tag{A.4}$$

This expression can be subdivided in two integrals

$$I_1 = \int_{\theta_1}^{\theta_2} \left[\frac{DK}{H\cos\theta + L\,\mathrm{sen}\,\theta} \right] d\theta \tag{A.5}$$

$$I_2 = \int_{\theta_1}^{\theta_2} \left[\frac{K^2(A\cos\theta + B\,\mathrm{sen}\,\theta)}{2(H\cos\theta + L\,\mathrm{sen}\,\theta)^2} \right] d\theta. \tag{A.6}$$

Integral term I_1 can be solved by means of the new two variables

$$E = \sqrt{H^2 + L^2}, \quad \varphi = \arctan\frac{H}{L}.$$

In this way, the simple function $\sin(\theta+\varphi)$ appears as a denominator so that

$$I_1 = \frac{DK}{E}\left(\ln\tan\frac{\theta_2+\varphi}{2} - \ln\tan\frac{\theta_1+\varphi}{2} \right). \tag{A.7}$$

Integral I_2 can be simplified by writing

$$\begin{aligned} A\cos\theta + B\sin\theta = {} & (A\sin\varphi + B\cos\varphi)\sin(\theta+\varphi) \\ & + (A\cos\varphi - B\sin\varphi)\cos(\theta+\varphi) \end{aligned} \tag{A.8}$$

so that

$$\begin{aligned} I_2 &= J_1 + J_2 \\ &= \int_{\theta_1}^{\theta_2} \frac{M}{\sin^2(\theta+\varphi)}\,d\theta + \int_{\theta_1}^{\theta_2} \frac{N\cos(\theta+\varphi)}{\sin^2(\theta+\varphi)}\,d\theta \end{aligned} \tag{A.9}$$

where

$$M = \frac{K^2(A\sin\varphi + B\cos\varphi)}{2E^2}$$

$$N = \frac{K^2(A\cos\varphi - B\sin\varphi)}{2E^2}$$

from which

$$J_1 = M\left(\ln\tan\frac{\theta_2+\varphi}{2} - \ln\tan\frac{\theta_1+\varphi}{2} \right) \tag{A.10}$$

$$J_2 = N\left(\frac{1}{\sin(\theta_1+\varphi)} - \frac{1}{\sin(\theta_2+\varphi)} \right) \tag{A.11}$$

and so all the terms of the singular coefficient are computed.

ACKNOWLEDGMENT

The authors wish to thank Dr. M. Iacomi for the help given in the analytical computation of singular integrals.

REFERENCES

[1] K. Reichert, "The calculation of magnetic circuits with permanent magnets by digital computers," *IEEE Trans. Magn.*, vol. 6, pp. 283–288, June 1970.

[2] M. J. Newman, L. R. Turner, and C. W. Trowbridge, "GFUN an interactive program as an aid to magnet design," in *Proc. 4th Magnet Technology Conf.*, Brookhaven, NY, 1972.

[3] R. Albanese and G. Rubinacci, "Integral formulation for 3D eddy current computation using edge elements," in *Proc. Inst. Elect. Eng.*, vol. 135, Nov. 1988, pp. 493–500.

[4] L. Kettunen and L. R. Turner, "A volume integral formulation for nonlinear magnetostatics and eddy currents using edge elements," *IEEE Trans. Magn.*, vol. 28, pp. 1629–1632, Mar. 1992.

[5] M. Gimignani, A. Musolino, and M. Raugi, "Integral formulation for nonlinear magnetostatic and eddy currents analysis," *IEEE Trans. Magn.*, vol. 30, pp. 3024–3027, 1994.

[6] A. Kalimov and M. Svedentsov, "Application of hybrid integro-differential method for analysis of thin magnetic shields," *IEEE Trans. Magn.*, vol. 34, pp. 2453–2456, 1998.

[7] R. Albanese and G. Rubinacci, "Finite element methods for the solution of 3D eddy current problems," in *Advances in Imaging and Electro Optics*. New York: Academic, 1998, vol. 102, pp. 1–86.

[8] A. Bossavit, "Whitney forms: A class of finite elements for three dimensional computations in electromagnetism," in *Proc. Inst. Elect. Eng.*, vol. 135, Sept. 1988, pp. 457–462.

[9] A. Gibbons, *Algorithmic Graph Theory*. Cambridge, U.K.: Cambridge Univ. Press, 1984.

[10] G. Drago, M. Repetto, G. Secondo, and J. Simkin, "A code for inductance computations in ironless structures," in *Proc. 4th IGTE Symp.*, Graz, Austria, Oct. 10–12, 1990, pp. 205–210.

[11] C. J. Collie, "Magnetic fields and potentials of linearly varying current or magnetization in a plane bounded region," in *Proc. COMPUMAG*, Oxford, U.K., Mar. 31–Apr. 2 1976, pp. 86–95.

[12] G. R. Cowper, "Gaussian quadrature formulas for triangles," *Int. J. Numer. Method Eng.*, vol. 8, pp. 256–258, 1972.

[13] I. D. Mayergoyz and G. Bedrosian, "On calculation of 3-D eddy currents in conducting and magnetic shells," *IEEE Trans. Magn.*, vol. 31, pp. 1319–1324, May 1995.

[14] F. I. Hantila, "Mathematical models of the relations between B and H for nonlinear media," *Rev. Roum. Sci. Tech.*, no. 3, pp. 429–448, 1974.

[15] M. Chiampi, A. Negro, and M. Tartaglia, "A finite element method to compute three-dimensional field distribution in transformer cores," *IEEE Trans. Magn.*, vol. 16, pp. 1413–1419, Nov. 1980.

[16] M. Chiampi, M. Repetto, and D. Chiarabaglio, "An improved technique for nonlinear magnetic problems," *IEEE Trans. Magn.*, vol. 30, pp. 4332–4334, Nov. 1994.

[17] M. Chiampi, D. Chiarabaglio, and M. Repetto, "An accurate investigation on numerical methods for nonlinear magnetic field problems," *J. Magn. Magn. Mater.*, vol. 133, pp. 591–595, 1994.

[18] O. Bottauscio, M. Chiampi, D. Chiarabaglio, and M. Zucca, "Use of grain oriented materials in low frequency magnetic shielding," *J. Magn. Magn. Mater.*, vol. 216, pp. 130–132, 2000.

Aldo Canova was born in Biella, Italy, in 1967 and received the degree in electrical engineering and the Ph.D. in electrical engineering from the Politecnico di Torino, Torino, in 1992 and 1996, respectively.

Since October 1995, he has been a Researcher with the Department of Industrial Electrical Engineering, Politecnico di Torino. He is involved in research activities related to the numerical computation of electromagnetic fields in the area of power devices.

Dr. Canova is a member of the Comitato Elettrotecnico Italiano (CEI) on the Technical Committee on rotating machines.

Maurizio Repetto (M'97) was born in Genova, Italy, in 1960, and received the degree and the Ph.D. degree in electrical engineering from University of Genova in 1985 and 1989, respectively.

He was a Researcher with the University of Genova from 1990 to 1992. In 1992, he joined the Politecnico di Torino, where he is now Full Professor of Fundamentals of Electrical Engineering. His main research interests are related to the numerical computation of electromagnetic fields in the area of power devices. In particular, he is involved in research projects about the analysis of ferromagnetic hysteresis and the automatic optimization of electromagnetic devices.